scientific reports

Check for updates

OPEN

Enhanced visualization of nuclear staining and cell cycle analysis for the human commensal *Malassezia*

Jayaprakash Sasikumar, Suparna Laha, Bharati Naik & Shankar Prasad Das✉

Malassezia **is a lipophilic commensal yeast that resides mainly on the mammalian skin and is also found to associate with the internal organs. Dysbiosis of** ***Malassezia*** **is related to several diseases and often escapes detection as it is difficult to culture and maintain.** ***Malassezia*** **cell wall differs from other budding yeasts like** ***S. cerevisiae*** **due to the difference in the lipid content and is difficult to transform. In this study, we present a methodology to stain** ***Malassezia's*** **nucleus and perform cell cycle studies. However, staining presents a challenge due to its exceptionally thick cell wall with high lipid content, hindering conventional methods. Our novel methodology addresses this challenge and enables the staining of the** ***Malassezia*** **nucleus with a low background. This would allow researchers to visualize the overall nuclear health specifically nuclear morphology and analyze DNA content, crucial for cell cycle progression. By employing DNA-specific dyes like DAPI or Hoechst, we can observe the nuclear structure, and using PI we can differentiate cells in distinct cell cycle phases using techniques like flow cytometry. This novel staining methodology unlocks the door for in-depth cell cycle analysis in** ***Malassezia*** **which has challenged us through ages being refractory to genetic manipulations, paving the way for a deeper understanding of this commensal fungus and its potential role in human health.**

Keywords *Malassezia*, Nuclear staining, Cell cycle, DAPI, Propidium iodide, Nocodazole, Zymolyase, FACS

Nuclear staining holds a fundamental significance in the realm of cell biology and plays a vital role in diverse applications like cell cycle analysis, DNA damage assays checking for chromatin integrity, genetic research, and the exploration of cellular structures. While it is considered a straightforward procedure in mammalian and other yeast cells, standard staining methods prove ineffective in the fungi *Malassezia*[1]. In nature, the commensal *Malassezia* is a genus of lipophilic fungi that is associated with warm-blooded animals. In humans, it is one of the microbes that is now known to be present in a wide range of organs, and in some of them like mouth, skin, and gut, it shows unique predominance and usually remains undetected due to difficulties in culture conditions and there are several barriers to studying this fungus such as slow growth, specific nutritional requirements[2], difficulties in revival[3], and lipid-rich cell walls[4] making it difficult for genetic manipulations[5]. *Malassezia* is widely considered a commensal organism[6], however in certain instances due to its immunomodulatory properties[7] and because of possible host genetic defects[8], it is implicated in a spectrum of diseases[9], spanning skin conditions from Seborrheic and Atopic dermatitis, Pityriasis versicolor, and Malassezia folliculitis[10,11], to chronic ailments such as Crohn's disease, Ulcerative colitis, and several cancers such as Pancreatic Ductal Adenocarcinoma, Cervical, Colorectal and Oral cancers[12–14]. Additionally, our recent study provided evidence of its coexistence with other fungi, which might exacerbate its pathogenicity towards severe infections[15]. Earlier research showed it to be the primary inhabitant of the epidermal region but recent findings revealed its presence in multiple organs of the human body[16–23]. Intriguingly, several *Malassezia* species and their DNA have been found in the brain of individuals[24–27], particularly in patients with neurodegenerative disorders[21,28–31], highlighting its potential pathogenic role in such conditions[32]. In addition to its pathogenic potential associated with yeast-to-hyphal conversion[33], dysbiotic populations of this fungus have been implicated in numerous diseases, emphasizing the critical need for deeper exploration of this commensal. Particularly, investigations into its associations with several cancers highlight the complexity of this commensal microbe.

Cell Biology and Molecular Genetics, Yenepoya Research Centre, Yenepoya (Deemed to Be University), Mangalore 575018, India. ✉email: shandas76@gmail.com

Recent technological advancements are gradually overcoming the hurdles and illuminating the true nature of these fungi. Hence, there is a need for more studies to explore this wolf in sheep-clothing pathogen[11,14]. As part of the ongoing investigation, a novel methodology has been developed to unveil *Malassezia*'s genome through nuclear staining. To achieve this, specific agents targeting the nucleus, like DAPI (4',6-diamidino-2-phenylindole) and Hoechst dyes are utilized which are traditionally used for nuclear staining. Both DAPI and Hoechst bind DNA by intercalating between base pairs, causing fluorescence enhancement upon binding[34,35]. Their distinctive blue fluorescence emission allows for specific visualization of DNA in cells, making them a widely used fluorescent stain for nuclear and chromosomal studies. DAPI has a preference for AT-rich regions of DNA due to the presence of more accessible grooves in these regions whereas Hoechst binds to GC-rich regions[36,37]. Moreover, Hoechst dyes are frequently used in conjunction with other fluorescent markers to distinguish between cell populations or identify subcellular structures, facilitating complex analyses such as immunofluorescence (IF) and fluorescence in situ hybridization (FISH)[38,39]. In addition to nuclear staining, an attempt was made to analyze the cell cycle of *Malassezia*. For this, Propidium iodide (PI) holds significant importance in nuclear staining and cell cycle analysis owing to its distinctive properties. PI is used to stain dead cells as live cells can flush out PI which doesn't happen in the case of DAPI[40]. As a fluorescent dye, PI selectively binds to DNA by intercalating between base pairs, emitting red fluorescence upon binding[41]. This property makes PI an excellent choice for nuclear staining, allowing for visualization and quantification of DNA content within cells. In cell cycle analysis, PI thus serves as a vital tool for discerning different cell cycle phases based on DNA content. By staining cells with PI and subjecting them to flow cytometry, researchers can accurately determine the proportion of cells in the different cell cycle phases, thus gaining insights into cell cycle progression and dynamics[42]. The cell cycle, a highly regulated process, consists of four main phases: G1 (gap 1), S (DNA synthesis), G2 (gap 2), and M (mitosis). Checkpoints tightly control progression through these phases, ensuring accurate DNA replication, repair, and cell division[43]. With the developed PI staining methodology for *Malassezia,* we tried to arrest the cells at a particular phase of the cell cycle, something that has not been attempted before. Various arresting agents, such as Nocodazole (targeting microtubule polymerization for metaphase arrest), hydroxyurea (blocking DNA replication for S phase arrest), and α-Factor (for arresting budding yeast at G1), are routinely used for cell-cycle-based studies. Nocodazole, a microtubule-depolymerizing agent, interferes with microtubule polymerization dynamics, leading to the disruption of the mitotic spindle apparatus and subsequent arrest of cells in mitosis. This arrest enables synchronization of cells at a specific cell cycle stage (G2/M), facilitating detailed analysis of molecular events and dynamics associated with that phase and also for studying effects in other cell cycle phases when cells are released into the cell cycle post-arrest[44]. For our methodology, we chose Nocodazole to arrest the cells at the G2/M transition which disrupts microtubule dynamics[45]. Microtubules are essential components of the cytoskeleton and play pivotal roles in various cellular processes, including chromosome segregation during mitosis[46]. By combining established methodologies with innovative techniques, our approach represents a significant step towards understanding cell biology and unraveling the complexities associated with the human commensal *Malassezia*.

Materials and methods

Materials and reagent preparation

25 mg of DAPI (Sigma) was dissolved in 1 ml of molecular-grade water and the stock solution was stored at − 20 °C. 40 µl from the 25 mg/ml DAPI stock solution was dissolved in 960 µl of molecular-grade water to make a working solution (1 mg/ml). This working solution was stored at 4 °C. 25 mg of Hoechst (Sigma) was dissolved in 1 ml of molecular-grade water and the stock solution was stored at − 20 °C. 40 µl from the 25 mg/ml Hoechst stock solution was dissolved in 960 µl of molecular-grade water to make a working solution (1 mg/ml). This working solution was stored at 4 °C. 10 mg of Zymolyase powder (MP Biomedicals) was dissolved in 1 ml of 0.1 M sodium phosphate solution and the stock solution (10 mg/ml) was stored at 4 °C. For 0.1 M Sodium phosphate solution 339.4 mg of sodium phosphate monobasic (HiMedia) and 2.021 g of sodium phosphate dibasic (HiMedia) were added with 80 ml of Milli-Q water. pH was adjusted to 7.4, volume made up to 100 ml, and stored at 4 °C. For 1X PBS solution, NaCl (0.8 g), KCl (20 mg), Na2HPO4 (0.114 g), and KH2PO4 (0.24 mg), were mixed with 80 ml of Milli-Q water. Volume was made up to 100 ml, autoclaved at 121 °C for 20 min, and stored at room temperature. The Triton X-100 solution was prepared by dissolving Triton X-100 in Milli-Q-Water at a 1:9 ratio. 1 mg of RNase powder was added to 1 ml of freshly prepared 1X PBS solution to prepare a stock solution (1 mg/ml) which was kept at − 20 °C. 100 µl from the 1 mg/ml RNase A stock was added to 900 µl of 1X PBS (100 µg/ml working solution) and stored at 4 °C. 1 mg of Propidium Iodide powder was dissolved in 1 ml of molecular-grade water, covered with aluminium foil, and stored at − 20 °C. 50 µl from the 1 mg/ml PI stock was dissolved in 950 µl of molecular-grade water (50 µg/ml working solution), covered with aluminium foil, and stored at 4 °C**.** The Cell Permeabilizing Solution (CP Solution) 545 µl, used per sample comprised 40 µl of Zymolyase (10 mg/ml), 500 µl of Triton X-100 solution, and 5 µl of β-mercaptoethanol. 10 mg of Nocodazole was mixed in 1 ml of DMSO to make a 10 mg/ml stock and stored at 4 °C until use. 25 mg of chloramphenicol is mixed in 1 ml of 95% ethanol to make a 25 mg/ml stock solution. Yeast cultures were grown in Sabouraud Dextrose (SD) media in an Incubator Shaker (Innova 44R, Eppendorf). Optical density was measured using a Digital photo colorimeter (Sky Technologies). Fluorescent images were captured using the fluorescence microscope (Oxion fluorescence, Euromex). Cell cycle analysis was done using the Flow cytometer (DxFlex, Beckman Coulter) and for data acquisition CytExpert (v2.6) was used. For flow cytometry data analysis Kaluza analysis (v1.6) was used and Adobe Illustrator (2023) was used for designing graphics and artwork.

Methods

Fungal growth

Malassezia pachydermatis (CBS 1879) cells (Westerdijk Fungal Biodiversity Institute, Utrecht, Netherlands) and *Saccharomyces cerevisiae* (699) cells[47] were streaked on an agar plate containing SD media with the addition of 50 µg/ml chloramphenicol to inhibit bacterial growth. The plate was then incubated at 32 °C for 3 days to facilitate the formation of distinct, visible single colonies. After the incubation period, a single fungal colony was selected and introduced into 5 ml of liquid SD media supplemented with 50 µg/ml chloramphenicol from the 25 mg/ml stock. This liquid culture was incubated overnight at 32 °C with shaking at 120 RPM in an incubator shaker. A subculture was initiated from the starter culture, adjusting the final concentration at OD_{600} of 0.1 in a liquid SD media supplemented with 50 µg/ml chloramphenicol. This subculture was allowed to grow until it reached an OD_{600} of 0.4–0.5. The resulting log-phase culture was employed for subsequent experimental procedures.

DAPI staining

To prepare *S. cerevisiae* cells for DAPI staining, 1 ml of culture with an OD_{600} of 0.4–0.5 was centrifuged at 5000 RPM for 5 min. The cells were then incubated with 70% ethanol for 30 min at room temperature. Following incubation, the cells were washed twice with 1X PBS, resuspended in 100 µl of 1X PBS, and vortexed. A 0.5 µg/ml DAPI/Hoechst solution was added, and the cells were incubated for 30 min at room temperature. After incubation, the cells were washed once with 1X PBS and observed under a microscope[48]. For *M. pachydermatis*, 1 ml of culture with OD_{600} of 0.4–0.5 was centrifuged at 5000 RPM for 5 min. The supernatant was discarded, and the pellet was resuspended in 1 ml of 1X PBS (pH 7.4) and vortexed. This suspension underwent centrifugation at the same conditions and duration, and the process was repeated twice. Following the PBS washes, the cell pellet was dissolved in 1 ml of 0.1N potassium phosphate solution (pH 7.4) and subjected to centrifugation. After discarding the supernatant, the pellet was resuspended in 1 ml of Triton X-100 solution and centrifuged. Following the removal of the supernatant, to the pellet 545 µl of CP solution (comprising of 500 µl Triton X-100, 40 µl of 10 mg/ml Zymolyase and 5 µl of β-mercaptoethanol (βME)) was added, mixed and incubated at 32 °C, 120 RPM in a shaking incubator for 2 h. After incubation, the cells were centrifuged, and the supernatant was discarded. The obtained pellet was washed once with Triton X-100 solution and once with 1X PBS buffer. Following these washes, post centrifugation the supernatant was removed, and the pellet was dissolved in 100 µl of 1X PBS. To the pellet, 1 µl of 1 mg/ml DAPI/ Hoechst solution was added and mixed. The cells with DAPI were incubated in the dark for 30 min at room temperature. After incubation, the cells were centrifuged, and the supernatant was discarded. The pellet was washed twice with Triton X-100 solution and then resuspended in 100 µl of 1X PBS. For observation, 10 µl of the stained cell suspension was taken and examined under an Oxion fluorescence microscope (Euromex) using a UV channel at 100X magnification.

Catalase, urease bile esculin, and viability test

Both the treated and the untreated (control) cells were checked for Catalase, Urease, and Bile esculin tests as performed in[49] to confirm that the cells are metabolically active. To evaluate the viability of cells following the treatment, the control (untreated) and treated cells were counted and plated onto SD plates. Viable colonies were counted and plotted as percent viable cells based on the average of two independent experiments.

Cell cycle arrest. 0.5 ml of the budding yeast cultures (OD_{600} of 0.4–0.5) were taken and to that 15 µg/ml nocodazole solution was added from 10 mg/ml stock and mixed well. This mixture was kept in a shaking incubator for 6 h at 32 °C for *M. pachydermatis* and 3 h for *S. cerevisiae* which are approximately two doubling times and kept at 120 RPM. After nocodazole incubation, the culture was taken and mixed with an equal volume of 70% ethanol and incubated at 4 °C overnight. After ethanol incubation, the mixture was centrifuged at 5000 RPM for 5 min, and the supernatant was discarded. The pellet was then washed twice with 1 ml of 1X PBS. After the washing steps, the cells were resuspended in 500 µl of PBS and supplemented with 100 µl of 100 µg/ml RNase A. The mixture was incubated at 50 °C in a dry bath for 1 h. Following the RNase treatment, 200 µl of 50 µg/ml PI solution was added, and the mixture was incubated at room temperature in the dark for 30 min.

Flow cytometry. The PI-stained cell suspension was diluted 1/10th using 1X PBS. The diluted cell suspension was loaded into the flow cytometer (Cytoflex, Beckman Coulter) sample tube. Data was acquired by running the samples through the flow cytometer at a suitable flow rate ranging between 250 and 500 cells/second, ensuring a minimum of 5000 events were recorded for reliable analysis. Appropriate laser and filter settings were selected for detecting PI fluorescence, as PI typically emits red fluorescence upon excitation by a blue laser. Firstly, cell populations were gated based on Forward Scatter-Area (FSC-A) and Side Scatter-Area (SSC-A) to exclude debris and select single cells in the FSC-A vs. SSC-A plot. Then, a plot of Forward Scatter-Area (FSC-A) vs. PI fluorescence filter-Area (PE-A) was created, and a gate was delineated to include only PI-positive cells. Subsequently, a histogram of PI fluorescence intensity (PE-A) vs. cell count for the PI-positive gated population was generated. The acquired data was further analyzed using flow cytometry software (Kaluza 1.6).

Results and discussion

We have developed a methodology for nucleus staining in *Malassezia*, something which was attempted earlier but didn't find much success[1]. Due to its thick cell wall, *Malassezia* is refractory to genetic manipulation as direct transformation is still a challenge. New genera are still being discovered with the help of next-generation sequencing technologies[50,51]. To investigate *Malassezia* cell biology initially, we employed standard yeast DNA staining protocols with DAPI and Hoechst[48,52–54], using the test strain *Malassezia pachydermatis* (CBS 1879) and *Saccharomyces cerevisiae* 699 strain as control. Subsequently, the cultured cells were ethanol-fixed, washed,

stained with DAPI or Hoechst, and subjected to microscopic examination. The standard staining method yielded clear nuclear visualization in the budding yeast *S. cerevisiae* (Fig. 1a). However, upon adhering to this procedure, a prominent stained nucleus is not observable in *Malassezia*, as the dye components tend to adsorb to the cell wall, resembling whole-cell staining rather than highlighting the nucleus (Fig. 1b). Repeated washing of the cells led to the removal of the whole cell staining giving a ghost-like appearance (Supplementary Fig. 1a) confirming the fact that DAPI tends to adsorb to the cell wall instead of entering into the cells, with the conventional protocol. This non-specific binding of DAPI may be attributed to its interaction with membrane lipids (phospholipids), as indicated in previous studies[55]. Given that phospholipids are major components of the *Malassezia* cell membrane[56] it strengthens the understanding of why DAPI staining in *Malassezia* can lead to increased non-specific fluorescence. Therefore, we developed a new staining method to visualize the *Malassezia* nucleus involving multiple standardization steps (Supplementary Fig. 2). This revised methodology involves growing yeast cells in SD media, pelleting, and washing them with PBS and potassium phosphate solution to remove the impurities. To permeabilize the cell walls, a key step in this procedure involves incubation with Zymolyase, which facilitates cell wall disruption by enzymatically cleaving β-1,3-glucan linkages, effectively weakening the fungal cell wall structure[57], along with βME, that promotes the action of Zymolyase. Then these partially permeabilized cells were washed with PBS to remove the traces of the enzyme because prolonged exposure to Zymolyase leads to damage to cellular integrity. Finally, the cells were treated with DAPI. This method partially reduced the non-specific staining compared to cells treated with the conventional protocol but prominent nucleus was still not observed (Fig. 2a). When employing the Triton X-100 solution, a non-ionic detergent, which can disrupt cell membranes, enhancing permeability and lipid dissolution[58] instead of Zymolyase also led to similar results (Fig. 2b). To enhance the effect of specific staining of the nucleus, we next incubated the cells with both Zymolyase, βME, and Triton X-100 (which we termed Cell Permeabilization or CP solution) to ensure proper permeabilization of the cells (Fig. 2c) which yielded better results than the individual treatments. Further to give enhanced visualization (clarity of the nucleus against low background staining) we washed the cells with Triton X-100 twice to obtain a distinct, prominent nuclei (Fig. 3a,b). In this case, Hoechst is more prone to photobleaching (2–3 s) compared to DAPI (5–6 s). So preferably DAPI can be a better choice for observing *Malassezia* nucleus using this methodology.

DAPI facilitates the visual observation of the nucleus, while an alternative DNA staining method utilizing Propidium Iodide (PI) not only aids in nuclear DNA visualization but also serves as a valuable tool for cell cycle analysis. PI-stained cell cycle analysis involves measuring the DNA content to distinguish the three main phases: G1, S, and G2/M. In G1, cells have a haploid DNA content, while the S phase is characterized by DNA synthesis and an increase in DNA content. G2/M marks the preparation for cell division with a diploid DNA content[59]. Through flow cytometry analysis, the distinct DNA content in each phase can be quantified by the intensity of PI fluorescence, allowing us to assess the distribution of cells across the cell cycle. In this regard, we have taken the growing culture of *M. pachydermatis* in SD media and an equal amount of ethanol was added to serve as a fixative for preserving the cellular structures. After this treatment, cells underwent RNase treatment to selectively degrade RNA, preventing interference with DNA fluorescence signals and ensuring accurate measurement of DNA. Subsequently, the RNase-treated cells were supplemented with PI staining to stain the DNA. This simplified method, utilizing minimal consumables, comparable to other cell cycle analysis protocols eliminates the need for additional reagents such as sodium citrate buffer and proteinase K[60,61] and has demonstrated reproducibility. We also analyzed the effect of this treatment on the cell viability. While the untreated cells showed no loss in viability, the treated cells using the new protocol showed nearly 50% viability. In addition, the treated cells using this new methodology were also found to be metabolically active as assessed from the Urease, Bile esculin, and Catalase tests (Supplementary Fig. 3). This will certainly add up newer avenues to do live cell imaging studies and other downstream applications using *Malasessia* as a host.

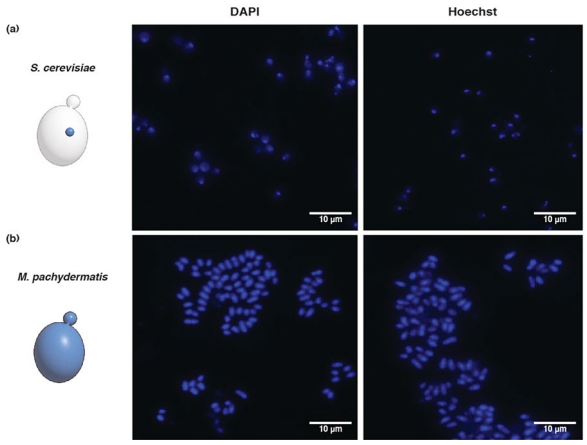

Figure 1. Comparison of nuclear staining profiles of yeasts using traditional methodology. Nucleus as observed in (**a**) *S. cerevisiae* and (**b**) *M. pachydermatis* using the stains DAPI and Hoechst.

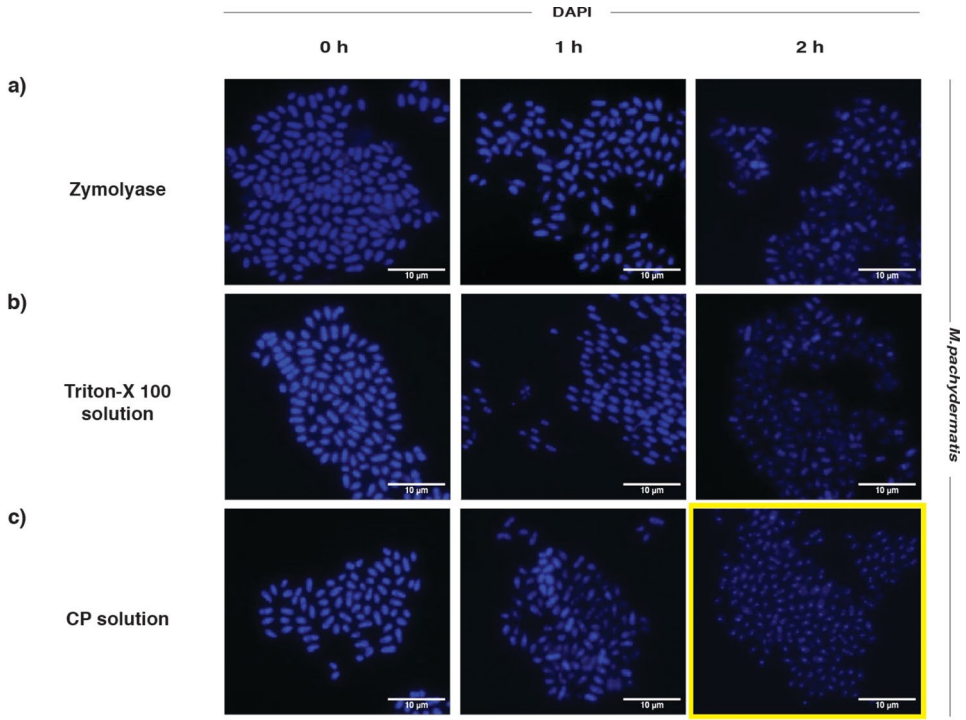

Figure 2. Critical elements contributing to the development of the novel methodology. DAPI staining using (**a**) Zymolyase, (**b**) Triton X-100 solution, and (**c**) both Zymolyase and Triton X-100 (CP solution). Treatment of the cells was carried out for 0, 1, and 2 h. The yellow highlighted box indicates the obtained distinct nucleus.

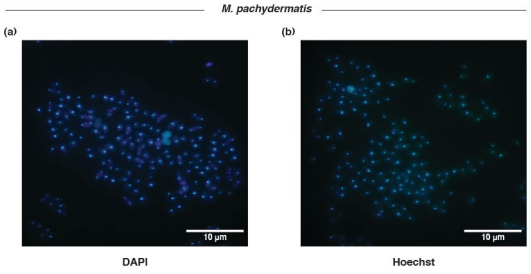

Figure 3. Nuclear staining profiles of *Malassezia* using the novel methodology. Nuclear staining protocol for *M. pachydermatis* using (**a**) DAPI and (**b**) Hoechst staining.

Having established PI staining methodology, we proceeded to undertake a novel and unprecedented task: cell cycle arrest in *Malassezia*, not reported before. These investigations involve synchronizing cells in different stages of the cell cycle, enabling a more precise analysis of molecular processes and events occurring at those specific stages. We used Nocodazole which is a microtubule-depolymerizing agent, that disrupts the dynamics of microtubule assembly and disassembly acting as a toxic agent inhibiting chromosome movement. It binds to tubulin and disrupts microtubule assembly/disassembly inhibiting mitotic spindle formation and chromosome segregation[44,62]. Therefore, we treated *M. pachydermatis* with nocodazole by adding it to the growing culture and allowed the cells to go through two doubling times. *S. cerevisiae* was taken as a positive control, to compare with *M. pachydermatis* (test). Upon treatment with nocodazole, the treated cells were stained with PI stain and observed under a microscope. The cells that responded to Nocodazole treatment arrest at the G2/M phase displayed distinctive characteristics, notably large buds with stained nuclei observed under a microscope Arrest of the *S. cerevisiae* cells happened in 2–3 h (Fig. 4a) but it was delayed in *Malassezia* to 5–6 h (Fig. 4b) because of its increased doubling time of approximately 3 h. Additional confirmation of cell cycle arrest was obtained through Fluorescence-activated cell sorting (FACS) analysis, revealing a prominent peak corresponding to the G2/M phase (Fig. 4 a,b).

While established methods for budding yeasts like *Saccharomyces* and *Candida* staining rely on their "permeable" cell walls, *Malassezia* demands a different approach since it has a lipid-rich thick cell wall (15–20%)[4] compared to *S. cerevisiae* having ~3% lipid content[63]. This novel method specifically targets the unique structure of the *Malassezia* cell wall and specifically stains the nuclear DNA, which remains unaffected by washing and

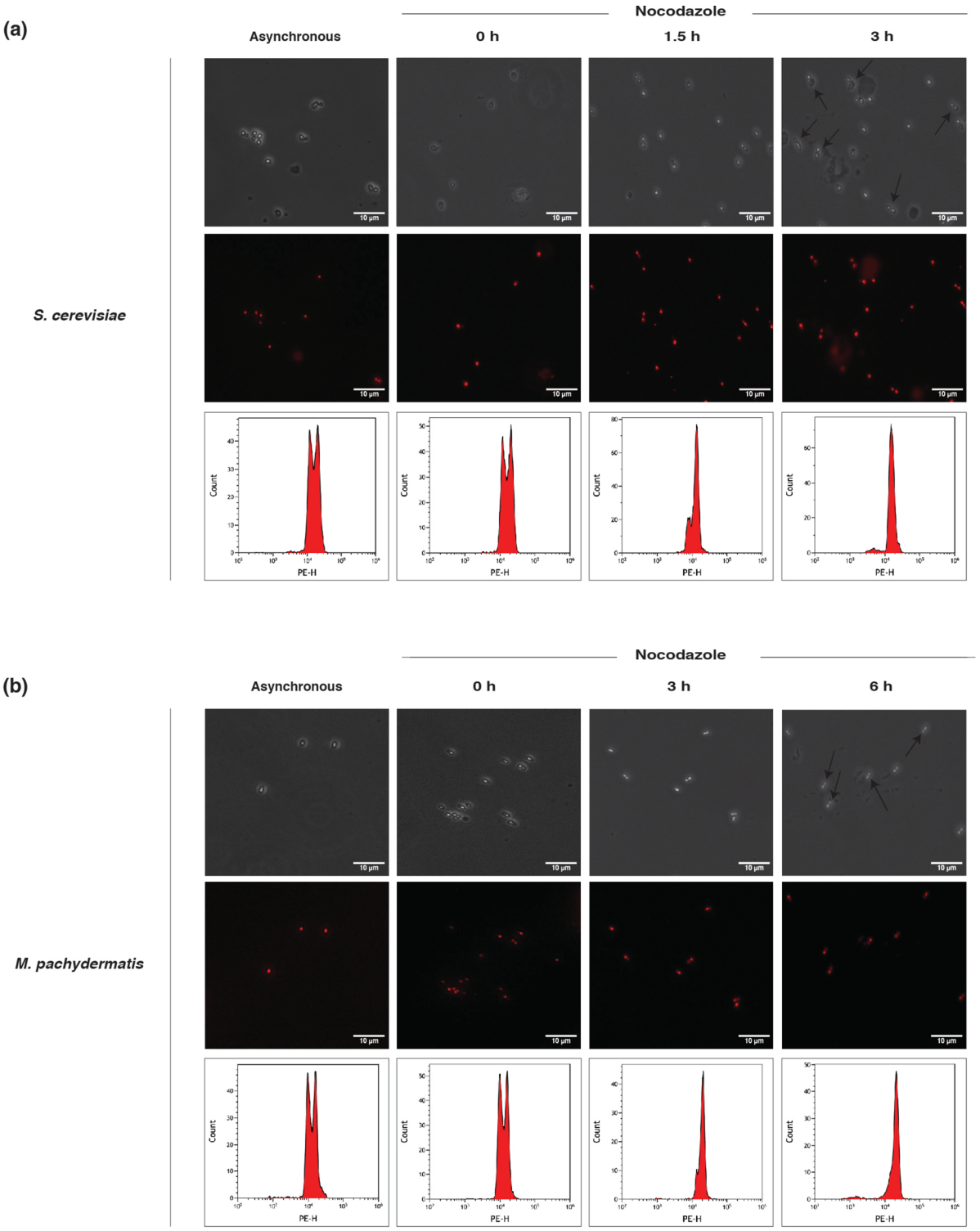

Figure 4. Cell cycle analysis of *Malassezia*. Microscopic images and FACS profiles illustrating cell cycle arrest induced by nocodazole in (**a**) *Saccharomyces cerevisiae* (asynchronous cells without nocodazole and cells treated with nocodazole for 0 h, 1.5 h, and 3 h) and (**b**) *Malassezia pachydermatis* (asynchronous cells without nocodazole and cells treated with nocodazole for 0 h, 3 h, and 6 h). Black arrows indicate large budded cells resulting from nocodazole-induced arrest.

quenching procedures (Supplementary Fig. 1b). By directly visualizing nuclear morphology and DNA content, researchers can now paint a detailed picture of the *Malassezia* cell cycle, unveiling the distribution of cells across different phases and identifying any potential disruptions or bottlenecks. Additionally, the ability to combine

this method with DNA-damaging agents opens doors to studying the response of *Malassezia* to genotoxic stress and associated DNA repair mechanisms, potentially paving the way for novel antifungal strategies. Especially, by shedding light on how *Malassezia* regulates its cell cycle, this research provides a sturdy groundwork for unravelling the intricate molecular events that drive cell division processes. Researchers can now delve into the molecular pathways and signalling cascades that orchestrate cell cycle transitions in *Malassezia*. The methodology has advantage of using minimal consumables, rendering them cost-effective and accessible for laboratories with limited resources. Most importantly this methodology provides improved specificity and clarity, enhancing the reliability of research outcomes. This reliability is crucial for scientific advancements, potentially accelerating discoveries and innovations that address health challenges, improve diagnostics, and inform therapeutic interventions.

Conclusion

In summary, we have provided a DNA staining methodology specifically tailored for fungi of the *Malassezia* genus, and similar fungi having thick cell walls, which is a challenging task due to their unique structural barriers. To overcome these obstacles, we employed a combination of enzymatic and chemical treatments to partially permeabilize their thick cell walls without significantly compromising their viability. This allowed us to successfully introduce DAPI and Hoechst dyes into the cells, enabling precise staining of the nucleus- an achievement not previously attained. In addition to this novel staining methodology, we undertook a cell cycle analysis of *Malassezia*. A brief timing steps associated with the protocol is presented in Supplementary Fig. 4 and we have also provided a troubleshooting guide for the users in Supplementary Table-1. Utilizing the cell cycle arresting agent Nocodazole, we were able to halt cells at the G2/M phase, as confirmed by both microscopy and FACS analysis. This pioneering work provides researchers with a direct visualization of the *Malassezia* nucleus and its cell cycle, facilitating the identification of its various phases. By combining this method with DNA damage-inducing agents, we can gain valuable insights into how *Malassezia* responds to genotoxic stress and repairs DNA, thereby opening avenues for novel antifungal strategies. Understanding the regulatory mechanisms governing the *Malassezia* cell cycle would lay the groundwork for unravelling the molecular events that drive cell division. This knowledge offers opportunities to explore molecular pathways and signalling cascades involved in cell cycle transitions, potentially revealing therapeutic targets for the regulation of *Malassezia* and related fungi.

Data availability

All data generated or analyzed during this study are included in this published article (and its Supplementary Information files).

Received: 9 May 2024; Accepted: 30 July 2024
Published online: 09 September 2024

References

1. Mittag, H. Fine structural investigation of Malassezia furfur: I Size and shape of the yeast cells and a consideration of their ploidy. *Mycoses* **37**, 393–399. https://doi.org/10.1111/j.1439-0507.1994.tb00388.x (1994).
2. Shetty, M., Naik, B. & Prasad Das, S. Rice bran oil supports robust growth of the commensal fungus *Malassezia*. *The Microbe* **3**, 100080. https://doi.org/10.1016/j.microb.2024.100080 (2024).
3. P.N. Brito, L.C. Paulino, Phylogenetic analysis reveals unexplored fungal diversity on skin, (2023) 2023.11.22.568368. https://doi.org/10.1101/2023.11.22.568368.
4. Billamboz, M. & Jawhara, S. Anti-malassezia drug candidates based on virulence factors of malassezia-associated diseases. *Microorganisms* **11**, 2599. https://doi.org/10.3390/microorganisms11102599 (2023).
5. Ianiri, G., Dagotto, G., Sun, S. & Heitman, J. Advancing functional genetics through agrobacterium-mediated insertional mutagenesis and CRISPR/Cas9 in the commensal and pathogenic yeast Malassezia. *Genetics* **212**, 1163–1179. https://doi.org/10.1534/genetics.119.302329 (2019).
6. Theelen, B. *et al.* Malassezia ecology, pathophysiology, and treatment. *Med. Mycol.* **56**, S10–S25. https://doi.org/10.1093/mmy/myx134 (2018).
7. Iliev, I. D. & Leonardi, I. Fungal dysbiosis: immunity and interactions at mucosal barriers. *Nat. Rev. Immunol* **17**, 635–646. https://doi.org/10.1038/nri.2017.55 (2017).
8. Naik, B., Ahmed, S. M. Q., Laha, S. & Das, S. P. Genetic susceptibility to fungal infections and links to human ancestry. *Front. Genet.* **12**, 709315. https://doi.org/10.3389/fgene.2021.709315 (2021).
9. Gaitanis, G., Magiatis, P., Hantschke, M., Bassukas, I. D. & Velegraki, A. The malassezia genus in skin and systemic diseases. *Clin. Microbiol. Rev.* **25**, 106–141. https://doi.org/10.1128/CMR.00021-11 (2012).
10. Saunte, D. M. L., Gaitanis, G. & Hay, R. J. Malassezia-associated skin diseases, the use of diagnostics and treatment. *Front. Cell Infect. Microbiol.* https://doi.org/10.3389/fcimb.2020.00112 (2020).
11. Bimbi, C., Lana, D., Kyriakou, G. & Wollina, U. Malassezia beyond tinea versicolor: the newest wolf in sheep's clothing pathogen?. *Cosmetic Med. Aesthet. Surg.* **44**, 4–12 (2023).
12. Abdillah, A. & Ranque, S. Chronic diseases associated with malassezia yeast. *J. Fungi (Basel)* **7**, 855. https://doi.org/10.3390/jof7100855 (2021).
13. Aykut, B. *et al.* The fungal mycobiome promotes pancreatic oncogenesis via MBL activation. *Nature* **574**, 264–267. https://doi.org/10.1038/s41586-019-1608-2 (2019).
14. Das, S. P., Ahmed, S. M. Q., Naik, B., Laha, S. & Bejai, V. The human fungal pathogen Malassezia and its role in cancer. *Fungal Biol. Rev.* **38**, 9–24. https://doi.org/10.1016/j.fbr.2021.08.002 (2021).
15. Naik, B., Sasikumar, J. & Das, S. P. Fungal coexistence in the skin mycobiome: a study involving Malassezia, Candida, and Rhodotorula. *AMB Expr* **14**, 26. https://doi.org/10.1186/s13568-024-01674-8 (2024).
16. Jayasudha, R. *et al.* Implicating dysbiosis of the gut fungal microbiome in uveitis, an inflammatory disease of the eye. *Investig. Ophthalmol. Vis. Sci.* **60**, 1384–1393. https://doi.org/10.1167/iovs.18-26426 (2019).
17. Gu, X., Cheng, X., Zhang, J. & She, W. Identification of the fungal community in otomycosis by internal transcribed spacer sequencing. *Front. Microbiol.* https://doi.org/10.3389/fmicb.2022.820423 (2022).
18. Cleland, E. J. *et al.* The fungal microbiome in chronic rhinosinusitis: richness, diversity, postoperative changes and patient outcomes. *Int. Forum Allergy Rhinol.* **4**, 259–265. https://doi.org/10.1002/alr.21297 (2014).

19. Dupuy, A. K. *et al.* Redefining the human oral mycobiome with improved practices in amplicon-based taxonomy: discovery of malassezia as a prominent commensal. *PLOS ONE* **9**, e90899. https://doi.org/10.1371/journal.pone.0090899 (2014).
20. Hammad, D. B. M., Liyanapathirana, V. & Tonge, D. P. Molecular characterisation of the synovial fluid microbiome in rheumatoid arthritis patients and healthy control subjects. *PLoS One* **14**, e0225110. https://doi.org/10.1371/journal.pone.0225110 (2019).
21. Pisa, D., Alonso, R. & Carrasco, L. Parkinson's disease: a comprehensive analysis of fungi and bacteria in brain tissue. *Int. J. Biol. Sci.* **16**, 1135–1152. https://doi.org/10.7150/ijbs.42257 (2020).
22. Ertam, I., Aytimur, D. & Alper, S. *Malassezia furfur* onychomycosis in an immunosuppressed liver transplant recipient. *IJDVL* **73**, 425. https://doi.org/10.4103/0378-6323.37067 (2007).
23. Kamamoto, C. S. L. *et al.* Cutaneous fungal microbiome: Malassezia yeasts in seborrheic dermatitis scalp in a randomized, comparative and therapeutic trial. *Dermato-Endocrinol.* https://doi.org/10.1080/19381980.2017.1361573 (2017).
24. Shek, Y. H., Tucker, M. C., Viciana, A. L., Manz, H. J. & Connor, D. H. Malassezia furfur—Disseminated infection in premature infants. *Am. J. Clin. Pathol.* **92**, 595–603. https://doi.org/10.1093/ajcp/92.5.595 (1989).
25. Rosales, C. M., Jackson, M. A. & Zwick, D. Malassezia furfur meningitis associated with total parenteral nutrition subdural effusion. *Pediatr. Dev. Pathol.* **7**, 86–90. https://doi.org/10.1007/s10024-003-4030-5 (2004).
26. Olar, A. *et al.* Central nervous system involvement by malassezia restricta, an unusual fungal pathogen: a report of two cases (P01245). *Neurology* **78**, P01.245. https://doi.org/10.1212/WNL.78.1_supplement.P01.245 (2012).
27. Rogacheva, Y. *et al.* Invasive fungal infection of the central nervous system caused by rare yeast pathogen Malassezia spp. in patients with acute leukemia: case reports and literature review. *Sci. Notes Pavlov Univ.* **27**, 80–87 (2021).
28. Alonso, R., Pisa, D., Aguado, B. & Carrasco, L. Identification of fungal species in brain tissue from Alzheimer's disease by next-generation sequencing. *J. Alzheimers Dis.* **58**, 55–67. https://doi.org/10.3233/JAD-170058 (2017).
29. Alonso, R., Fernández-Fernández, A. M., Pisa, D. & Carrasco, L. Multiple sclerosis and mixed microbial infections. Direct identification of fungi and bacteria in nervous tissue. *Neurobiol. Dis.* **117**, 42–61. https://doi.org/10.1016/j.nbd.2018.05.022 (2018).
30. Alonso, R., Pisa, D., Fernández-Fernández, A. M., Rábano, A. & Carrasco, L. Fungal infection in neural tissue of patients with amyotrophic lateral sclerosis. *Neurobiol. Dis.* **108**, 249–260. https://doi.org/10.1016/j.nbd.2017.09.001 (2017).
31. Alonso, R., Pisa, D. & Carrasco, L. Brain microbiota in Huntington's disease patients. *Front. Microbiol.* https://doi.org/10.3389/fmicb.2019.02622 (2019).
32. Naik, B., Sasikumar, J. & Das, S. P. From skin and gut to the brain: The infectious journey of the human commensal fungus Malassezia and its neurological consequences. *Mol. Neurobiol.* https://doi.org/10.1007/s12035-024-04270-w (2024).
33. Li, J. *et al.* Presence of Malassezia hyphae is correlated with pathogenesis of seborrheic dermatitis, microbiology. *Spectrum* **10**, e01169-e1221. https://doi.org/10.1128/spectrum.01169-21 (2022).
34. Bucevičius, J., Lukinavičius, G. & Gerasimaitė, R. The use of hoechst dyes for DNA staining and beyond. *Chemosensors* **6**, 18. https://doi.org/10.3390/chemosensors6020018 (2018).
35. Kapuscinski, J. DAPI: a DNA-specific fluorescent probe. *Biotechnol. Histochem.* **70**, 220–233. https://doi.org/10.3109/10520299509108199 (1995).
36. Reddy, B. S. P., Sondhi, S. M. & Lown, J. W. Synthetic DNA minor groove-binding drugs☆. *Pharmacol. Therapeut.* **84**, 1–111. https://doi.org/10.1016/S0163-7258(99)00021-2 (1999).
37. Cho, J. & Rando, R. R. Specific binding of Hoechst 33258 to site 1 thymidylate synthase mRNA. *Nucleic Acids Res.* **28**, 2158–2163 (2000).
38. Siljak-Yakovlev, S., Pustahija, F., Vicic, V. & Robin, O. Molecular cytogenetics (FISH and fluorochrome banding): Resolving species relationships and genome organization. *Methods Mol. Biol.* **1115**, 309–323. https://doi.org/10.1007/978-1-62703-767-9_15 (2014).
39. König, K., Riemann, I., Fischer, P. & Halbhuber, K. J. Multiplex FISH and three-dimensional DNA imaging with near infrared femtosecond laser pulses. *Histochem Cell Biol.* **114**, 337–345. https://doi.org/10.1007/s004180000185 (2000).
40. Darzynkiewicz, Z., Li, X. & Gong, J. Chapter 2 assays of cell viability: Discrimination of cells dying by apoptosis. In *Methods in Cell Biology* (eds Darzynkiewicz, Z. *et al.*) 15–38 (Academic Press, Cambridge, 1994).
41. Atale, N., Gupta, S., Yadav, U. C. S. & Rani, V. Cell-death assessment by fluorescent and nonfluorescent cytosolic and nuclear staining techniques. *J. Microsc.* **255**, 7–19. https://doi.org/10.1111/jmi.12133 (2014).
42. Cecchini, M. J., Amiri, M. & Dick, F. A. Analysis of cell cycle position in mammalian cells. *JoVE* https://doi.org/10.3791/3491 (2012).
43. L. Ding, J. Cao, W. Lin, H. Chen, X. Xiong, H. Ao, M. Yu, J. Lin, Q. Cui, The roles of cyclin-dependent kinases in cell-cycle progression and therapeutic strategies in human breast cancer. Int. J. Mol. Sci. 21 (2020). https://doi.org/10.3390/ijms21061960.
44. Blajeski, A. L., Phan, V. A., Kottke, T. J. & Kaufmann, S. H. G1 and G2 cell-cycle arrest following microtubule depolymerization in human breast cancer cells. *J. Clin. Invest.* **110**, 91–99. https://doi.org/10.1172/JCI13275 (2002).
45. Endo, K., Mizuguchi, M., Harata, A., Itoh, G. & Tanaka, K. Nocodazole induces mitotic cell death with apoptotic-like features in *Saccharomyces cerevisiae*. *FEBS Lett.* **584**, 2387–2392. https://doi.org/10.1016/j.febslet.2010.04.029 (2010).
46. G.M. Cooper, Microtubules, in: The Cell: A Molecular Approach. 2nd Edition, Sinauer Associates, 2000. https://www.ncbi.nlm.nih.gov/books/NBK9932/ (accessed February 21, 2024).
47. Laha, S., Das, S. P., Hajra, S., Sau, S. & Sinha, P. The budding yeast protein Chl1p is required to preserve genome integrity upon DNA damage in S-phase. *Nucleic Acids Res.* **34**, 5880–5891. https://doi.org/10.1093/nar/gkl749 (2006).
48. D.H. Williamson, D.J. Fennell, [62] Visualization of yeast mitochondrial DNA with the fluorescent stain "DAPI". In: Methods in Enzymology, Academic Press, Cambridge, 1979: pp. 728–733
49. Naik, B., Sasikumar, J. & Das, S. P. Fungal coexistence in the skin mycobiome: a study involving Malassezia Candida, and Rhodotorula. *AMB Exp.* **14**, 26. https://doi.org/10.1186/s13568-024-01674-8 (2024).
50. Cho, Y.-J., Yang, J., Shin, S.Y., Kim, H.K., Rintarhat, P., Park, M., Sung, M., Lagree, K., Underhill, D.M., Lee, D.-W., Choi, C.H., Yang, C.-S., Jung, W.H. Live Malassezia strains isolated from the mucosa of patients with ulcerative colitis, (2023) https://doi.org/10.1101/2023.11.28.569113.
51. Kashaf, S. S. *et al.* Integrating cultivation and metagenomics for a multi-kingdom view of skin microbiome diversity and functions. *Nat. Microbiol.* **7**, 169–179. https://doi.org/10.1038/s41564-021-01011-w (2022).
52. Amberg, D. C., Burke, D. J. & Strathern, J. N. Yeast vital stains: DAPI stain of nuclear and mitochondrial DNA. *Cold Spring Harb Protoc* https://doi.org/10.1101/pdb.prot4163 (2006).
53. A. Cone, Yeast DAPI Staining, (2016). https://www.protocols.io/view/Yeast-DAPI-Staining-eigbcbw (accessed January 30, 2024).
54. Sazer, S. & Sherwood, S. W. Mitochondrial growth and DNA synthesis occur in the absence of nuclear DNA replication in fission yeast. *J. Cell Sci.* **97**, 509–516. https://doi.org/10.1242/jcs.97.3.509 (1990).
55. Favilla, R., Stecconi, G., Cavatorta, P., Sartor, G. & Mazzini, A. The interaction of DAPI with phospholipid vesicles and micelles. *Biophys. Chem.* **46**, 217–226. https://doi.org/10.1016/0301-4622(93)80015-B (1993).
56. A.M. Celis Ramirez, Unraveling lipid metabolism in lipid-dependent pathogenic Malassezia yeasts, (2017). https://dspace.library.uu.nl/handle/1874/356776 (accessed September 5, 2023).
57. Scott, J. H. & Schekman, R. Lyticase: Endoglucanase and protease activities that act together in yeast cell lysis. *J. Bacteriol.* **142**, 414–423 (1980).
58. Thomas, D. S., Ingham, E., Bojar, R. A. & Holland, K. T. In vitro modulation of human keratinocyte pro- and anti-inflammatory cytokine production by the capsule of Malassezia species. *FEMS Immunol. Med. Microbiol.* **54**, 203–214. https://doi.org/10.1111/j.1574-695X.2008.00468.x (2008).

59. Nair, A. & Manohar, S. M. A flow cytometric journey into cell cycle analysis. *Bioanalysis* **13**, 1627–1644. https://doi.org/10.4155/bio-2021-0071 (2021).
60. Rosebrock, A. P. Analysis of the budding yeast cell cycle by flow cytometry. *Cold Spring Harb Protoc* https://doi.org/10.1101/pdb.prot088740 (2017).
61. S.K. Patel, S.R. Sahu, N. Acharya, Cell cycle analysis of candida Albicans by flow cytometry, Bio. Protoc. 13 (2023) e4848. https://doi.org/10.21769/BioProtoc.4848.
62. Santangelo, G., Navari, S. & Bruno, P. A highly specific microtubule depolymerizing agent (nocodazole) affecting meiosis activation in the protozoan Blepharisma japonicum (Ciliata, Heterotrichida), Italian. *J. Zool.* **64**, 227–234. https://doi.org/10.1080/11250009709356201 (1997).
63. Suomalainen, H. & Nurminen, T. The lipid composition of cell wall and plasma membrane of baker's yeast. *Chem. Phys. Lipids* **4**, 247–256. https://doi.org/10.1016/0009-3084(70)90026-5 (1970).

Author contributions

SPD conceptualized, reviewed, and approved the manuscript. JS contributed towards writing, revision, and providing critical suggestions and artwork. SL helped in FACS, revising the manuscript. BN helped in the initial standardization and review of the manuscript.

Funding

The authors would like to acknowledge funding from the Indian Council of Medical Research (ICMR) in New Delhi, INDIA for funding our research program. SPD is supported by the DHR Grant GIA/2019/000620/PRCGIA/2020-ECD II. JS is supported by a junior research fellowship from Yenepoya (Deemed to be University). The authors would like to thank Yenepoya Research Centre for the laboratory facilities and the Department of Oncopathology, Yenepoya (Deemed to be University) for the FACS.

Competing interests

The authors declare no competing interests.

Additional information

Supplementary Information The online version contains supplementary material available at https://doi.org/10.1038/s41598-024-69024-z.

Correspondence and requests for materials should be addressed to S.P.D.